ANALYSIS AND IMPLEMENTATION OF AN ORIENTATION-AWARE SOURCE LOCALIZATION SYSTEM WITH SMART DEVICES

A Thesis

by

DANIEL ANTONIO TUÑÓN CORONADO

Submitted to the Office of Graduate and Professional Studies of
Texas A&M University
in partial fulfillment of the requirements for the degree of

MASTER OF SCIENCE

Chair of Committee,	Jean-François Chamberland
Committee Members,	Gregory H. Huff
	Krishna R. Narayanan
	Radu Stoleru
Head of Department,	Chanan Singh

August 2014

Major Subject: Electrical Engineering

ABSTRACT

Target localization in wireless systems has experienced a great improvement during recent years given the increasing demand for location services by mobile users. Particularly, localization methods based on received signal strength indicator (RSSI) are highly attractive because hardware is readily available and cost-effective.

The RSSI-based localization literature generally focuses on the propagation environment sensitivity and overlooks a major factor in signal strength variability: the relative orientation between the source and the receiver. With current advancements in hardware, especially low-cost microelectromechanical sensors, most wireless devices are orientation-aware. This offers an opportunity to enhance the performance of multi-agent localization systems.

We propose to include orientation knowledge and the typical antenna radiation pattern asymmetries of the sensing devices into the inference task. We will gather experimental data using Android™ smartphones as sensing devices, implement the new orientation-aware algorithm and asses the improvements of our approach in simulations and real-world scenarios.

We compare the new scheme with the standard setting where the orientation is unknown. The orientation-aware implementation performs significantly better than the traditional systems in terms of accuracy. These results show that orientation-awareness capabilities should be accounted for whenever possible in tasks of statistical inference. Furthermore, this idea is likely to find applications beyond source localization.

DEDICATION

To my family and Melissa

ACKNOWLEDGEMENTS

I would like to express my deepest gratitude to my advisor, Dr. Jean-François Chamberland, for his guidance and continuous support throughout the course of this research. I appreciate his patience, motivation, enthusiasm, immense knowledge and especially the confidence he had in me. I could not have imagined having a better advisor and mentor for my studies.

My sincere thanks also goes to Dr. Gregory Huff, whose experience in the practical issues was invaluable. I am grateful to his team at the Wireless Communications Laboratory, particularly to Travis Taghavi, for their help and knowledge sharing. I would also like to thank the rest of my committee members, and the faculty and staff of the Department of Electrical Engineering at Texas A&M University.

I must recognize the support of the Panamanian Government through the "Professional Excellence Scholarship Program" administered by IFARHU-SENACYT. Without their support, my graduate studies would not have been possible.

I wish to express my gratitude to my friends and colleagues for making my time at Texas A&M University a great experience. Last and foremost, I want to thank my family, who have always supported me.

TABLE OF CONTENTS

Page

LIST OF FIGURES

FIGURE Page

LIST OF TABLES

TABLE Page

1. INTRODUCTION AND LITERATURE REVIEW

Target localization in wireless systems refers to the problem of accurately estimating the positions of devices. This topic has been an active research area for years due to its importance and wide range of applications. In this paradigm, receivers measure signal parameters such as connectivity, signal strength, angle of arrival and/or time of arrival [1] [2]. In general, cooperative localization can drastically increase system performance in terms of both accuracy and coverage [1]. Many algorithms have been proposed to perform such tasks. Consequently, it is not surprising to find much literature about the different approaches for target and multi-target localization in wireless sensor networks (WSNs) [3]. Such networks also introduce new challenges given the limited amount of resources available at the sensor nodes. These constraints include limitations on the amount of information that can be exchanged between sensors to achieve a desired level of performance, the computational power dedicated to cooperative signal processing, and the energy that can be used for computation and communication [4] [5].

Historically, direction finding and target localization technology have been used extensively for aero and maritime navigation and for military purposes such as the location of illegal, secret or hostile transmitters [6]. In recent years, wireless location technology has become a key feature for emergency aid and disaster response. It is widely deployed on aircraft, vessels and places prone to avalanches [7]. When needed, an emergency beacon transmits a unique identification signal that can aid in finding the exact location of the source. Other applications involve radio frequency interference detection and wildlife tracking [8]. Over the last decade, a lot of attention has been given to this area, especially after the Federal Communications

Commission (FCC) introduced the wireless enhanced 911 (E911) location-accuracy rules [9]. These rules aim to improve the accuracy and reliability of wireless 911 calls, thereby enabling public safety and emergency personnel to respond more efficiently and effectively. This requires all wireless carriers to take steps to provide more precise automatic localization information, specifically the latitude and longitude coordinates of an emergency 911 call. In addition to emergency services, there is an increasing interest in using smart antennas to improve system capacity and expand cellular communication coverage area [10]. In this latter setting, the objective is to develop an efficient algorithm to control an adaptive antenna that can direct the maximum radiation toward the intended destination without creating undue interference to other users. Furthermore, location services create new commercial opportunities for location motivated products such as mobile advertising or location-based wireless access security [9].

Over the past few years, we have witnessed the rapid development of advanced mobile technology driven by the advent of the smartphone. Smartphone technology supports real-time communication and information access, and it offers powerful and portable computing capabilities with the potential to generate a direct impact on human development. The global smartphone adoption rate has skyrocketed, growing faster than any consumer technology in history [11] [12] and demanding an improved manufacturing process. As a result, mass production processes for this technology have drastically decreased the cost of high-quality components. Examples of elements that have benefited from the smartphone revolution include batteries, accelerometers, gyroscopes and compasses. Consequently, it is now reasonable to assume that advanced wireless sensors have access to similar technology and hence are orientation aware. This, coupled with the asymmetrical radiation pattern characteristics of many devices, provides an opportunity for enhanced wireless localization perfor-

mance relying on existing technology. Notably, the Android™ operative system plays an important role in the mobile industry because it allows manufacturers to produce quality devices without worrying about software. This makes development cheaper and gets devices in the hands of more people. The wide availability of a free, multiplatform mobile operating system is a game changer for mobile application developments. The Android software development kit (SDK) offers a rich set of application programming interface (API) libraries and developer tools necessary to build, test, and debug Android apps.

Overall, the growing demand for accurate localization capabilities for current and future applications, coupled with the mobile technology effervescence, sets the way for the vast ongoing research in this area. Regarding its implementation, target localization faces challenges, as every other wireless implementation, intrinsic to the wireless environment. This makes finding the accurate location of an object a difficult task. Wireless phenomena include channel fading, interference, low signal-to-noise ratios (SNRs), and multipath conditions [13]. They pose several interesting problems from a signal processing perspective, and small errors in acquisition can lead to large errors in location estimates. Signal parameters are crucial in developing accurate localization systems. Hence, it is fundamental to learn the propagation characteristics of the medium. Propagation analysis provides a good initial estimate of the signal characteristics. There are two main approaches to channel modeling described in the literature, deterministic models and stochastic models [13]. The deterministic approach, mostly based on ray tracing, describes the channel behavior on the basis of physical laws, site geometry and known or assumed electrical parameters [14]. They provide accurate predictions of a system performance in a static environment. On the other hand, the stochastic approach implies extracting a statistical profile from channel responses gathered during an extensive measurement campaign [14]. For outdoor

wireless systems, this has been the preferable approach, producing several models that are considered crucial and indispensable tools for various applications [14].

Over the years, many approaches for localization algorithms have been proposed in the literature. They can be divided into two categories: range-based and range-free approaches [3]. They differ in the information used for the localization task. The selection of an approach depends on the application requirements.

Range-free approaches estimate the location by exploiting the radio connectivity information, or proximity, among nearby sensing nodes and anchor nodes with known position [15]. They were conceived to overcome limitations such as hardware cost and energy expenditure of the range-based localization schemes. Because of their simplicity, they are considered an effective and low-cost alternative for use in resource-constrained environments such as wireless sensor networks. However, these solutions suffer from low accuracy and their efficacy is a function of the density of the deployed anchor nodes [15]. Important localization techniques based on range-free approach include Centroid, APIT, Multidimensional Scaling Map (MDS-MAP), DV-HOP and Ad-Hoc Positioning System. In addition to the localization schemes mentioned above, many more have been proposed.

Range-based approaches require distance or angle information to accurately assess the location of an unknown device. Their high accuracy is very desirable in localization. However, such algorithms require more sophisticated hardware, are computationally expensive and are subject to uncertainties associated with transmission media and environmental features [16]. The measurements employed for the estimation process could be any physical reading that indicates distance or relative position. They are typically angles of arrival or directions of arrival, times of arrival, time differences of arrival or received signal strengths between the source and receiver. The angles of arrival can be obtained by measuring the difference in re-

ceived phase between antenna array elements at the receiver [8]. By combining the angles of arrival estimates of all receivers, an estimate of the target position can be obtained. Beside the typical sources of error, such as noise and interference, angles of arrival observations are sometimes corrupted by non-line-of-sight (NLOS) effects and errors in the angular orientation of the installed antenna arrays [9]. Time based methods, times of arrival and time differences of arrival record the propagation time when arriving at different receivers. This can be directly translated into distances, based on the known signal propagation speed [2]. The measured time of arrival is the time of transmission plus a propagation-induced time delay. The transmitter-receiver separation distance can then be directly calculated from the time delay as signals propagate with a know velocity. One successful implementation of this scheme is the Global Positioning System (GPS), which is known to provide global location information with a relatively high degree of accuracy, down to a few meters. Still, this technology can be expensive in terms of cost, and battery consumption. Here, the mobile station receives and measures the signal parameters from four or more satellites in the GPS satellite network. The parameter measured for each satellite is the time the satellite signal takes to reach the mobile station [9]. One drawback of methods based on times of arrival is that they require accurate synchronization between the receivers and source clocks so that time measurements translate directly into precise distances rather than time differences of arrival measurements where clock synchronization is avoided [9]. The received signal strength, commonly known as RSS, measures the power level being received by the antenna [8]. Devices can measure it during normal data communication and this paradigm does not require additional bandwidth or energy. Such schemes are fairly simple and inexpensive to implement. RSS exploits the relation among power loss and the distance between a source and the destination. In free space, signal power decays with the square of

the distance between the transmitter and receiver [13]. In terrestrial channels, signal decay differs by environment due to multipath signals and shadowing effects. This characteristic of high sensitivity to the propagation environment makes RSSI-derived distance estimates prone to very large errors at large path lengths, leading many researchers to conclude that RSS is an unreliable method for localization. However, a weighted approach can be implemented to fully utilize the accuracy of the range measurements made by the closest devices [17]. Furthermore, some researchers have recently focused on the estimation of the power-distance gradient or the path-loss exponent jointly with localization [18].

The estimation of the direction-of-arrival of a narrowband source is the simplest scenario in a localization context. In the general case, there is no closed-form solution which implies that a numerical search method is needed. Estimation techniques are divided into three different types: conventional techniques, subspace based techniques and maximum likelihood techniques. Conventional methods are founded on the concepts of beamforming and null steering [19] and do not exploit the statistics of the received signal. Example of these methods are the delay-and-sum method (DAS) [20] and the Capon Minimum Variance method [21], where several sets of complex weights can be applied to the antenna elements. The delayed signals are summed and the power is computed. The direction is then determined by analyzing the peak of the output power spectrum from all sets of complex weights. On the other hand, subspace-based direction finding methods exploits the underlying data model of narrow-band signals in additive noise [22]. This is the basis of Multiple Signal Classification (MUSIC) [23] and Estimation of Signal Parameters via Rotational Invariance Techniques (ESPRIT) [22] algorithms. Subspace estimation techniques are based on the eigenvalue decomposition of the spatial covariance matrix. This decomposition results in the formation of the signal and noise subspaces. Embedded

in the signal subspace is the information about where the signals are, while the noise subspace indicates where they are not [24]. Maximum Likelihood (ML) techniques have also been widely used and investigated [25] [26]. Problems involving maximum likelihoods are less popular than suboptimal subspace techniques because of the computational intensive load of the multivariate nonlinear maximization [21]. However, its high resolution in the determination of parameters such as incident angle, propagation delay and complex amplitude resulted in techniques derived from maximum likelihood principles with reduce computational load and capable to achieve faster convergence rates. One of them is the Alternating Projection (AP) algorithm [21], based on an iterative technique that transforms the multivariate nonlinear maximization problem, involved in the Maximum Likelihood estimator, into a sequence of simpler one-dimensional maximization problems. Another closely related method is the Space Alternating Generalized Expectation maximization (SAGE) algorithm [27], which generalizes the Expectation-Maximization (EM) algorithm's idea of data augmentation steps to reduce computational complexity. Rather than estimating all parameters directly, SAGE breaks down one high-dimensional problem into several low-dimensional ones and uses the EM principle to sequentially update the parameter subsets corresponding to each reduced problem while holding the others fixed [28]. As mentioned before suboptimal techniques with reduced computational load have dominated the field. However, in terms of performance, maximum likelihoods techniques are superior to subspace techniques, especially in low signal-to-noise ratio conditions [28].

This thesis explores both theoretically and practically how information on sensors orientation can improve the operation of a RSS-based multi-agent localization system, mainly assessing the gains associated with orientation-aware algorithms in determining the location of a source. This idea comes from the fact that the re-

ceived signal strength (RSS) does not only dependent on the distance and channel attenuation between the source and the receiver, but also on the effective antenna gain product of their respective orientations. If we assume the source to be omni-directional, its orientation becomes inconsequential. Contrastingly, due to a variety of form factors and other design or operational characteristics, wireless devices embedded antennas are subject to directional patterns and thus the orientation of the sensing device matters. Fig. 1.1 illustrates the effect of rotation on a directional antenna. Overall, the device orientation has a high influence on the received sig-

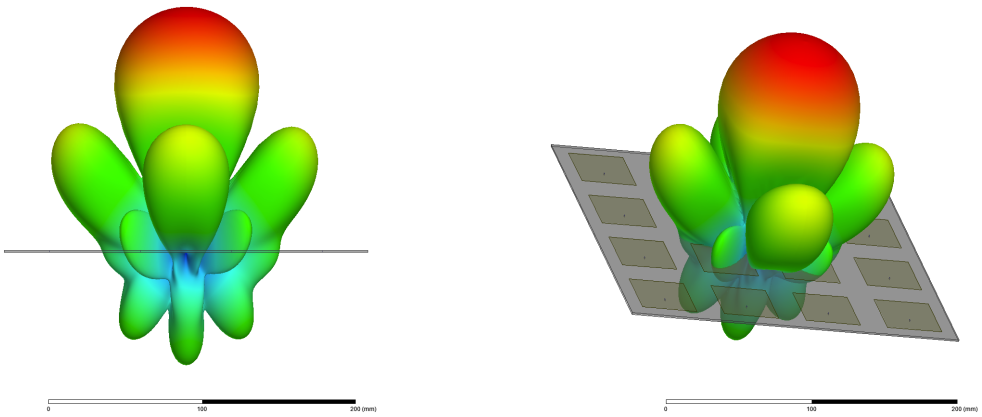

Figure 1.1: Effective antenna gain due to rotation.

nal strength used for the estimation process [29]. Orientation have been study in some scenarios for range-free localization where the emphasis is on improving a radio frequency fingerprinting technique [30]. Nevertheless, in much of the literature on range-based localization, this effect is not take into account by itself, instead it is omitted, or tied to the stochastic models variations associated to the shadowing effects. Exploiting access to a device's orientation and combining its directional antenna profile, an algorithm could translate the extra information into better overall

performance.

With this concept in mind, we set up a basic framework consisting of multiple sensing nodes, represented by Android™ smartphones, trying to pinpoint the localization of a single omnidirectional source in an outdoor environment using Wi-Fi technology. The received signal strength indicator (RSSI) and orientation information is gathered at every sensing node through the wireless network interface controller and embedded sensors such as GPS, accelerometer and compass. An Android application, developed using API libraries, is installed on each device to acquire and manage the aforementioned data. Observations are subsequently stored in an external database service for further joint analysis. This schema requires a centralized server system in charge, not only of holding information, but also of running the estimation algorithms. For estimation purposes, two RSSI-based localization algorithms using Maximum Likelihood Estimator are implemented; with one of them taking into account the orientation of the sensing device. It is important to mention that both algorithms require certain knowledge of the environmental path-loss model and the new algorithm also requires the antenna profile of each sensing device; this latter information is collected prior to deployment.

Finally, a quantitative analysis is done to asses both algorithms using localization error as a performance metric to establish whether the proposed approach is beneficial or not.

2. RSS-BASED LOCALIZATION

RSS-based localization methods are attractive because they only require simple hardware and low network overhead. These methods are based on a standard feature found in many wireless devices: a received signal strength indicator (RSSI). This ensures that a broad range of transceivers can be used. However, we must emphasize that there is no standardized relationship between RSSI values and the power level received by the antenna [29]. Consequently, the RSSI reported is highly dependent on the manufacturer and several publications suggest caution about using RSSI readings for distance estimation. Nevertheless, we can still take advantages of the information embedded in these readings to obtain estimates under proper calibration. Throughout this thesis, we assume that the RSSI is proportional to the power ratio in decibels of the measured power referenced to one milliwatt (dBm).

RSS-based localization generally uses an estimate of the distance between the emitter and receiver as a primary entity for determining position. This is obtained from a model describing the relationship between received power and distance. The localization problem consists then of estimate the source coordinates using every sensor location and likely distance to the transmitter. Intuitively, the more sensors found in an area, the more accurate the estimation should be.

In a wireless environment, the received signal power is not only vulnerable to noise, interference, antenna orientation and other channel obstacles such as multipath propagation, fading and shadowing, but these obstacles change over time in unpredictable ways [13]. Consequently, RSS does not only depend on distance, but on a multitude of factors. As such, a proper channel model is extremely important and must take all these factors in consideration. The following sections present

the mathematical model and tools available in literature that will be used for the estimation process in our wireless system.

2.1 Wireless Communication Channel

The wireless radio channel poses a great challenge as a medium for reliable communication. As mentioned before, accurately modeling the behavior of the wireless channels is essential. Fluctuations in link quality are commonly modeled as a combination of path loss, shadowing, and multipath fading. Path loss is caused by the dissipation of the power of an RF signal propagating through space as well as the effects of the propagation channel [13]. Models take this effect into account through the path loss exponent (PLE), which defines the rate at which the signal power decays over distance. Typical values range between 2 and 4 depending on the environment, and it has to be experimentally determined [31]. Shadowing is caused by obstacles between the transmitter and receiver that affects the wave propagation, attenuating the signal power through absorption, reflection, scattering, and diffraction [31]. Multipath fading occurs when multiple transmission paths are combined either constructively or destructively at the receiver, as a result of the transmitted signal reflection on objects before reaching the destination [13]. Multipath causes rapid changes in the RSS that are generally smaller in magnitude than shadowing.

Numerous channel models have been proposed for indoor and outdoor radio environments, some more accurate and complex than others. An attractive channel model for RSS-based localization, given its simplicity, is the lognormal shadowing path loss model; yet other models such as Rayleigh fading and Ricean fading can also be used [31]. Detailed information about channel modeling for wireless communication can be found in [19].

A common representation of a wireless environment is given by $r(t) = g(d)s(t) +$

$w(t)$, where $r(t)$ represents the received waveform, $s(t)$ is the sent signal, and $g(d)$ denotes the aggregate channel gain as a function of distance. In this equation, $w(t)$ captures additive Gaussian noise. Variations in power gain, $G(d) = |g(d)|^2$, are governed by several factors including the mean path loss, shadow fading and antenna gain.

The received power for a given distance between transmitter and receiver, assuming a lognormal channel model, can be expressed as

$$P(d)[\text{dB}] = A + B\log_{10}(d) + L_{\text{s}} + G_{\text{a}}, \tag{2.1}$$

where A is a combination of the transmitted signal power and a reference path loss and B represents ten times the path loss coefficient. Variable L_{s} is an independent and identically distributed (iid) Gaussian random variable representing shadow fading, $L_{\text{s}} \sim \mathcal{N}(0, \sigma_{\text{s}}^2)$ and G_a designates the antenna gain. We note that the mean of L_{s} can be absorbed in A. Thus, without loss of generality, we assume that the shadow fading component has mean zero. Site-specific values for A and B can be acquired by applying an estimation method to a reasonably large sample [32].

Several classes of random variables can be employed to model shadow fading, most notably the log-normal and gamma distributions. Herein, we select the log-normal density function. Thus, in the logarithmic domain, we get

$$f_{L_{\text{s}}}(\ell; \mu_{\text{s}}, \sigma_{\text{s}}^2) = \frac{1}{\sqrt{2\pi}\sigma_{\text{s}}} \exp\left(-\frac{\ell - \mu_{\text{s}}}{2\sigma_{\text{s}}^2}\right). \tag{2.2}$$

Paralleling the discussion above, we set $\mu_{\text{s}} = 0$. The variance parameter can be estimated through a measurement campaign; the unbiased sample variance is subse-

quently given by [33]

$$\sigma_{\mathrm{s}}^2 = \frac{1}{n-1}\sum_{k=1}^{n}\left(\ell_k - \mu_{\mathrm{s}}\right)^2, \tag{2.3}$$

where n is the sample size, $\{\ell_k\}$ forms the data set, and points are expressed in the logarithmic domain.

The objective of the estimation methods is to find the parameters associated to a mathematical model that best describes a set of data points, in a way that the model and the data are as close as possible. The most common estimation approach is the least squares method, which minimizes the sum of the squares of the offsets or residuals (a residual being the difference between an observed value and the fitted value provided by a model). The least square method as defined in (2.1) is given by

$$(A, B) = \underset{a,b}{\operatorname{argmin}} \left\| \underbrace{\begin{bmatrix} p_1 \\ \vdots \\ p_n \end{bmatrix}}_{\mathbf{p}} - \underbrace{\begin{bmatrix} 1 & \log_{10}(d_1) \\ \vdots & \vdots \\ 1 & \log_{10}(d_n) \end{bmatrix}}_{M} \begin{bmatrix} a \\ b \end{bmatrix} \right\|^2 \tag{2.4}$$

where p denotes received power at distance d. Then, the optimal coefficients are given by

$$\begin{bmatrix} a \\ b \end{bmatrix} = (M^{\mathrm{H}}M)^{-1}M^{\mathrm{H}}\mathbf{p}. \tag{2.5}$$

The variance of L_{s}, the shadow fading component, is computed by normalizing the residual error,

$$\sigma_{\mathrm{s}}^2 = \frac{1}{n-1}\mathbf{p}^{\mathrm{H}}\left(I - M(M^{\mathrm{H}}M)^{-1}M^{\mathrm{H}}\right)\mathbf{p} \tag{2.6}$$

where M is the linear regression matrix defined above.

2.2 Localization Estimation Problem

Our localization task is to estimate the position of an emitter using a network of collaborative sensors. The location may be computed relatively to one another, producing a relative localization; or with respect to the global coordinate system, yielding an absolute localization.

There exist several RSS-based localization methods. A well known range-free approach is the Radio Frequency Fingerprint, where the source location is determined by best matching the obtained RSSI values to a pre-recorded radio map. This radio map is constructed in a training phase or offline phase and it contains the measured RSSI at different locations [34]. Techniques for finding the best match include k-nearest neighbor, Euclidean distance, neural networks, and Bayesian statistics.

Range-based approaches used the RSSI information as a reference for distance and, subsequently, a geometric interpretation or a probabilistic framework to estimate the source location. The RSS lateration algorithm, a geometric approach, relies on the fact that this problem is equivalent to pinpointing a location in a 2D or 3D Cartesian coordinate system. Any point can be defined by distances to a set of known coordinates, i.e., the intersection of three circles. Figure 2.1 illustrates this concept. However, the possible errors in the resulting distance estimate cause ambiguity in the circle intersections and other methods to minimize the error must be used.

A stochastic framework considers the problem of signal processing in the presence of random noise. Herein, the localization is a statistical analysis to estimate the position of the source based on a distance estimate from RSS measurements under the assumed noise model of log-normal shadowing given by (2.1).

Most localization algorithms use models that do not account for antenna characteristics and their effects on received signal strength. Indeed, it is common to find

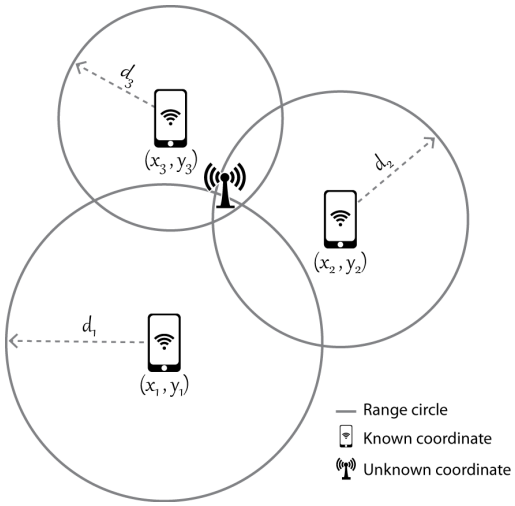

Figure 2.1: Lateration techniques use the geometry of circles to determine the source position.

scenarios where the antenna gain is omitted or implicitly integrated into the variations produced by the environment. In contrast, our approach considers the antenna impact. In the absence of orientation information, we assume that the random antenna gain obeys a log-normal distribution with expected value $\exp(\sigma_{\mathrm{a}}^2/2)$. In the logarithmic domain, this corresponds to a zero-mean normal random variable with variance σ_{a}^2. The noise level is estimated using the unbiased sample variance, as in (2.3).

The estimation in a stochastic framework is often based upon the principle of maximum likelihood. The maximum likelihood estimator (MLE) chooses as its solution the parameter that maximizes the likelihood of the observed data [32].

The likelihood of the distance is given by

$$l(d|p) = \frac{1}{\sqrt{2\pi(\sigma_{\mathrm{s}}^2 + \sigma_{\mathrm{a}}^2)}} \exp\left(-\frac{(p - A - B\log_{10}(d))^2}{2(\sigma_{\mathrm{s}}^2 + \sigma_{\mathrm{a}}^2)}\right). \tag{2.7}$$

In practice, it is frequently more convenient to work with the logarithm of the like-

lihood function, known as the log-likelihood function, which is equal to

$$\mathcal{L}(d|p) = -\frac{\ln 2\pi(\sigma_{\mathrm{s}}^2 + \sigma_{\mathrm{a}}^2)}{2} - \frac{(p - A - B\log_{10}(d))^2}{2(\sigma_{\mathrm{s}}^2 + \sigma_{\mathrm{a}}^2)}. \tag{2.8}$$

Since logarithm is a monotonic, continuously increasing function, the value which maximizes the log-likelihood function will also maximize its likelihood function. The maximum likelihood estimator for the location of the source, under the assumption that the noise components are independent, is given then by

$$\hat{\mathbf{x}} = \underset{\mathbf{x}_0}{\operatorname{argmax}} \sum_{k=1}^{n} \mathcal{L}\left(d(\mathbf{x}_0, \mathbf{x}_k)|p_k\right) \tag{2.9}$$

where $\mathbf{x}_k$ is the known position of sensor k, $\hat{\mathbf{x}}$ is the estimated position of the source and $d(\cdot,\cdot)$ represents Euclidean distance. In this expression, variable $\mathbf{x}_0$ ranges over the set of possible locations.

2.3 Performance Evaluation

Once the localization algorithm is in place, a quantitative measurement of performance is necessary. We will use the empirical mean distance error as a method to quantify the difference between values implied by an estimator and the true values. The distance error is defined as an Euclidean distance, that is the length of a line segment connecting the true target location and the estimated location obtained from the algorithm. Mathematically, the empirical mean distance error is given by

$$\bar{\mathrm{d}}(\underline{\hat{\mathbf{x}}}, \underline{\mathbf{x}}) = \frac{1}{n}\sum_{i=1}^{n} \|\underline{\hat{\mathbf{x}}}_i - \underline{\mathbf{x}}_i\|_2 \tag{2.10}$$

where $\hat{\mathbf{x}}$, the estimate parameter, and $\mathbf{x}$, the true value, are vectors representing locations in a two-dimensional space.

3. SYSTEM MODEL

3.1 Problem Statement

The system model consists of wireless links which connect the sensing devices to the source. Each sensing device is gathering three types of data: the received signal strength indicator (RSSI), the global positioning coordinates (GPS) and the relative orientation towards the magnetic north. The received power at a sensing device is governed by the fluctuations in link quality, which are commonly model through a combination of path loss and shadowing. We will use the approach introduced in Section 2.1 as reference for distance estimation. The global positioning coordinates will provide self-positioning for each sensor. The absolute orientation of the phone will be calculated from the inertial measurement unit embedded in the device. The inference task is to localize the wireless transmitter using the information provided by several distributed agents. The system model is shown in Fig. 3.1. Furthermore, we will characterize the overall performance of a source localization algorithm that takes into consideration the orientation of the sensing units.

3.2 Orientation

Determine the orientation of a device entails finding the rotation relative to a fixed frame of reference. Two coordinate systems are defined: the device coordinate system and the global coordinate system, which represents the reference system. We adopt the framework used in the Android software development kit (SDK) where the device's coordinate frame is define relative to the screen of the phone in its default orientation; that is, a portrait orientation. The x-axis points to the right, the y-axis points towards the top of the screen and the z-axis is perpendicular to the front of the screen, as shown in Fig. 3.2. It is important to understand that the sensor's

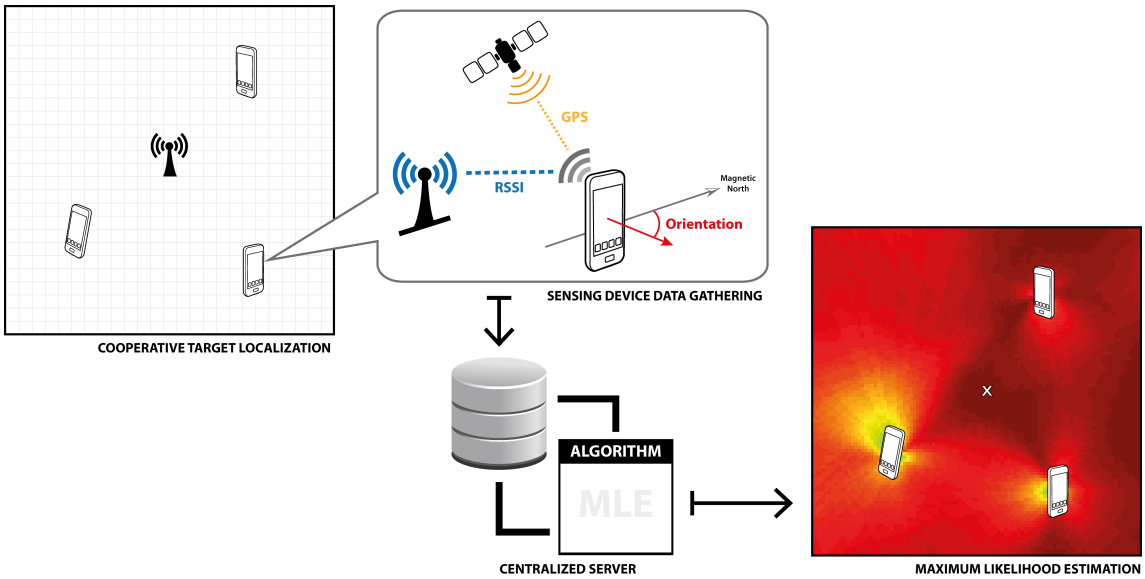

Figure 3.1: This figure illustrates the system model.

coordinate system never changes as the device moves.

The global coordinate system, or reference frame, is defined as a direct orthonormal basis. The z-axis points away from the center of the Earth and is perpendicular to the ground. The xy-plane is tangential to the Earth surface, with y-axis pointing towards the magnetic north and the x-axis pointing approximately East, as displayed in Fig. 3.2.

Methods to gain the orientation of moving objects using inertial measurement unit (IMU) components have been widely study in the field of Inertial Navigation Systems (INS). Nowadays, low-cost microelectromechanical sensors (MEMs) are integrated in many devices and can be used in several applications. Accelerometers can provide an acceleration vector associated with the phenomenon of weight experienced by the frame of reference, these measurements are given in meters per second squared. Magnetometers measure the ambient magnetic field in micro-Tesla, and gyroscopes

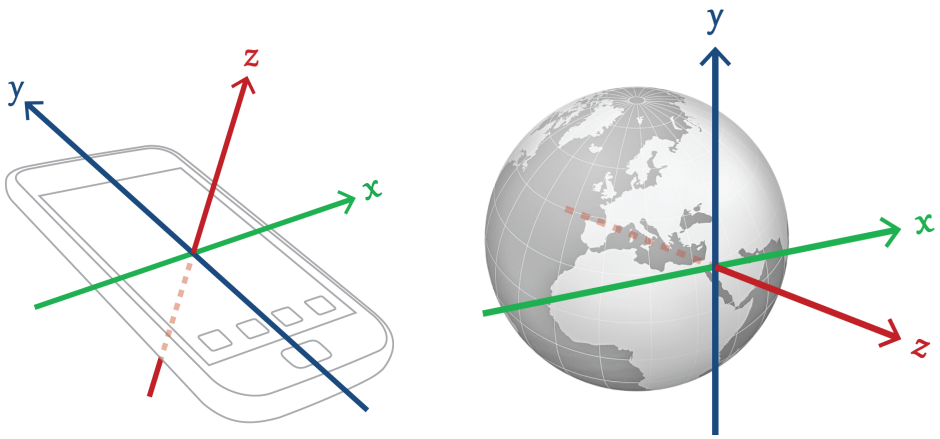

(a) Device's Coordinate System (b) Global Coordinate System

Figure 3.2: Reference frames

provide angular rotation speed in radians per second; all of them along the x-, y-, and z-axes of the device.

The device's orientation may be determined by the local fusion of accelerometer and magnetometer measurements. Still, both signals are prone to hardware noise and also the latter is subject to interference by electromagnetic activities nearby. In addition, orientation systems frequently use the gyroscope's sensitivity to increase reliability and accuracy. Orientation in gyros is derived by integrating the speed measurements over time to calculate a rotation angle. Although gyroscopes are more accurate, provide rapid response to angle changes and do not have interference problems, they are prone to bias and integration errors that introduce drift in the signal. Therefore, one must be cautions while using these values.

3.2.1 Overcoming Hardware Limitations

In practice, there are a few challenges to calculate the orientation, as mentioned before, due to hardware limitations. However, it is possible to minimize the drift and noise of the output orientation by implementing data fusion, thereby leveraging

gyroscope, magnetometer and accelerometer measurements. For instance, to obtain an accurate and responsive orientation, the gyroscope signal may only be applied for orientation changes in short time intervals, while the accelerometer and magnetic field signals are used over long periods of time. This is equivalent to high-pass filtering the gyroscope and low-pass filtering the accelerometer and magnetometer [35].

Additionally, magnetometer sensors are very sensitive to interference from local magnetic fields. Once they have been exposed to this interference over a prolonged period, the sensor will no longer be accurate and will need re-calibrating. User's help is needed for the calibration process. It is worth mentioning that new self-calibrating sensing technology is been developed and implemented. In the near future, calibration should no longer be a limitation.

3.3 Data Acquisition

RSSI and location information is accessible through the Android API functions. RSSI can be obtained per request through the `WifiManager` class. The geographic location is periodically updated using the GPS unit, and it can be access through the `LocationManager` class in GPS-enabled Android devices. In a similar fashion, the Android API offers very handy functions through the `SensorManager` class to get the absolute orientation. The common way to get this information is to use the `SensorManager.getOrientation()` method, whose outputs are three orientation angles, azimuth or yaw (rotation around z-axis), pitch (rotation around x-axis), and roll (rotation around y-axis). According to the Euler Theorem, the orientation of a rigid body can be uniquely defined by these three angles, also known as Euler angles. This Android API method is based on the output data from the accelerometer and magnetometer. The accelerometer provides the gravity vector, the vector pointing towards the center of the Earth, and the magnetometer functions as a com-

pass providing a vector that points to the magnetic north. The information from both sensors is enough to calculate the device's orientation. Note that the coordinate systems used in the `SensorManager.getOrientation()` method are differents, the x and z axes are inverted. Consequently, azimuth and pitch are positive in the clockwise direction for the regular device and world coordinate convention. Furthermore, to ensure a one-to-one mapping of all possible azimuth-pitch-roll angles to all possible orientations, one of the rotation angles must be restricted to a 180° range. In Android platforms, pitch is restricted to the range of $-90°$ to 90°. As an alternative, to increase accuracy, a new Java method for fusing gyroscope, accelerometer and magnetometer data can be implemented by using a Kalman Filter or the Direction Cosine Matrix (DCM) algorithm.

The Euler representation (azimuth-pitch-roll) is the simplest method to implement orientation, but contains ambiguities. These ambiguities are called gimbal locks. The rotation angles are uniquely determined except for the singular case when two of the three gimbals are driven into a parallel configuration, losing one degree of freedom in a three-dimensional mechanism. In our case, the difference of azimuth and roll is completely undetermined for a pitch of 90° or $-90°$, corresponding to an upright or a downward position, respectively. Slightly away from these pitch values, there is a unique solution, yet small changes in orientation may lead to large changes in azimuth and roll angles separately while keeping changes to the sum small. Usually, to avoid the gimbal lock problem, the transformation is represented using rotation matrices or normalized quaternions. Also supported through the Android API methods `SensorManager.getRotationMatrix()` and `SensorManager.getQuaternionFromVector()` respectively.

3.4 Simple Case Scenario: Orientation-Aware Localization

In a simplified scenario, we assume that the smartphone is in an up-right position, meaning pitch and roll will be fixed, and the device will only rotate in azimuth. Consequently, the relative orientation of the device with respect to the location of the source is represented by a single angle ϕ. Due to the gimbal lock problem mentioned above, the azimuth returned values using the `SensorManager.getOrientation()` API function will be prone to errors. Since we will only focus on one angle at this moment, we can use the function `SensorManager.remapCoordinateSystem()` to circumvent this issue. This provides a way to change the natural mapping between the Earth coordinate system and the device coordinate system. In our case, for instance, the z-axis of the phone will be mapped to the y-axis of the Earth and the azimuth will be calculated between these two axes, allowing precise measurements and avoiding the gimbal lock problem altogether.

3.4.1 Source Estimation

For orientation-aware devices, we use a stochastic framework similar to the one introduced in (2.8). We modify the log-likelihood function to include the orientation of the phone towards the source. In this case, the log-likelihood function is given by

$$\mathcal{L}(d|p,\phi) = -\frac{\ln 2\pi\sigma_{\mathrm{s}}^2}{2} - \frac{(p - A - B\log_{10}(d) - G_{\mathrm{a}}(\phi))^2}{2\sigma_{\mathrm{s}}^2}. \tag{3.1}$$

When the phone orientation is obtained from the internal sensors, the global MLE becomes

$$\hat{\mathbf{x}} = \underset{\mathbf{x}_0}{\operatorname{argmax}} \sum_{k=1}^{n} \mathcal{L}\left(d(\mathbf{x}_0, \mathbf{x}_k)|p_k, \phi_k\left(\mathbf{x}_0, \mathbf{x}_k, \phi_k'\right)\right) \tag{3.2}$$

where ϕ'_k denotes the absolute orientation of the Sensor k with respect to the global coordinate system. The relative orientation of the device with respect to a potential location $\mathbf{x}_0$ can be calculated, revealing ϕ_k, the proper argument to $G_{\mathrm{a}}(\cdot)$. This scenario can be better appreciated in Fig. 3.3.

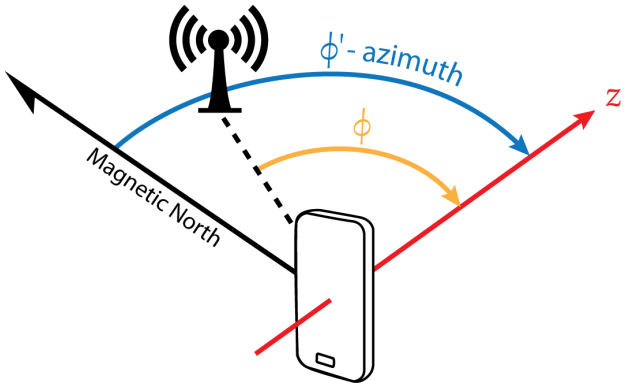

Figure 3.3: This figure illustrates the difference between the absolute orientation ϕ', obtained from the Android API and the relative orientation with respect to the source ϕ, the proper argument to $G_{\mathrm{a}}(\cdot)$.

3.4.2 Implementation

Our implementation uses a centralized scheme where all data is gathered in a single database and jointly processed. The localization algorithm is based on a maximum likelihood technique implemented in a MATLAB environment.

Two important considerations when implementing an orientation-aware source localization algorithm are: handling GPS coordinates and establishing a reference for orientation. First, we interpret the GPS data collected. The Global Positioning System (GPS) uses the World Geodetic System 1984 (WGS84). Geodetic systems or geodetic data are used to provide the real location of a point near the surface of the

Earth. In geodetic coordinates, locations are described in terms of latitude, longitude and height. These systems are needed because of the imperfect ellipsoid shape of the earth. This ellipsoid is completely parameterized by the semi-major axis and the flattening values showed in Table 3.1. In target applications, the local East,

Table 3.1: Constants from WGS84, the coordinate system used by GPS.

Parameter	**Value**
Earth semi-major axis	6378.137 km
Inverse flattening (1/f)	298.2572236

North, Up (ENU) Cartesian coordinate system is far more intuitive and practical than geodetic coordinates. The local ENU coordinate is formed from a plane tangent to a fixed point on the Earth's surface and uses linear X, Y and Z coordinates to locate elements with respect to the coordinate system origin. By convention the east axis is labeled X, the north Y and the up Z. Because it assumes a flat earth, it is not a good coordinate system to use over large distances. To perform the conversion from geodetic to Cartesian coordinates we rely on the database service implemented. The centralized server is running PostgreSQL, an open-source object-relational database management system (ORDBMS), and PostGIS a spatial database extender to add support for geographic objects. The data obtained from GPS is translated into a Cartesian coordinate system using the function `ST_Distance_Spheroid`, provided by PostGIS, which returns a linear distance between two latitude/longitude points given a particular spheroid.

Furthermore, we choose our reference for orientation and specified it into the algorithm. We know that sensors embedded in the sensing device provides orientation

with respect to the magnetic north and not the true or geographic north. Hence, we must decide what would be our reference point in the algorithm. To use true north as reference, we must apply a correction to compass directions. This correction, commonly known as magnetic declination, is the angle in degrees between the magnetic north and the true north. By convention positive means rotated east that much from true north. This adjustment could be done at the algorithm level or at the sensing application side. The Android API function `GeomagneticField.getDeclination()` provide the means to obtain the magnetic declination value. Alternatively, using the magnetic north as reference implies defining its geographic location in the algorithm. The fact is that the strength and direction of the Earth's magnetic field are constantly changing [36]. Consequently, the location of the geomagnetic poles are not fixed at specific geographic locations. They moves by a variable amount from day to day and year to year. However, they can be computed from a main field model, such as the World Magnetic Model (WMM) or the International Geomagnetic Reference Field (IGRF). Actually, the Android API function for declination uses the coefficients and formulas from the technical report: The US/UK World Magnetic Model for 2010-2015, provided by the National Oceanic and Atmospheric Administration (NOAA).

Finally, once the position of the sensing devices can be laid out in a Cartesian coordinate system and the absolute orientation is known, we run the inference task using the maximum likelihood estimators in (3.2), see Pseudocode 1.

Pseudocode 1 Orientation-aware source localization

1: **for all** k receivers **do**
2: transform GPS location (lat, lon) to Cartesian coordinates (x, y)
3: **for all** potential location $\mathbf{x}_0$ **do**
4: compute $d = \|\mathbf{x}_0 - \mathbf{x}_k\|$
5: transform absolute orientation, ϕ'_k, to relative orientation, ϕ, towards $\mathbf{x}_0$
6: calculate $loglikelihood[\mathbf{x}_0] = \mathcal{L}(d|p_k, \phi)$
7: **end for**
8: compute $cooperativeLoglikelihood \mathrel{+}= loglikelihood$
9: **end for**
10: calculate $\hat{\mathbf{x}} = \max(cooperativeLoglikelihood)$
11: **return** $\hat{\mathbf{x}}$

4. EXPERIMENTAL SETUP

4.1 Overview

Three measurement campaigns are necessary to assess the orientation-aware localization method proposed in this work. The first experiment gathers information to define the receiver's antenna gain as a function of its orientation. The second experiment seeks to provide statistical evidence for the wireless channel model adopted throughout. This model is used to determine the characteristics of the environment that are eventually used for numerical simulations. The third campaign aims to evaluate the orientation-aware localization algorithm with actual RSS data under real conditions.

This chapter details the way the experiments are designed, and explains the analysis of the gathered information.

4.1.1 Transmitter

The transmitter is a single-antenna access point with a transmit power of 16 dBm. The mounted monopole antenna provides an omni-directional, linear polarized pattern. The source transmits with a carrier frequency centered at 2.4 GHz. This band is part of the industrial, scientific and medical (ISM) radio bands and it is used by Wi-Fi technology.

4.1.2 Receivers

In our case, the sensing devices are embodied by Android™ smartphones. These devices feature Wi-Fi and GPS modules from which the status of the wireless network and global positioning information can be acquired. The orientation of the device is obtained using the built-in tri-axis accelerometer and compass components of the

inertial measurement unit (IMU).

We employed five commercial smartphones during the experiments, three HTC Evo™4G and two HTC ThunderBolt™. An Android application was developed and installed on each device to collect and store data locally. After each experiment and once the device is connected to the Internet the data is transferred to a central server.

4.2 Antenna Characterization

A proper characterization of the received signal strength as function of the device orientation is critical for the orientation-aware algorithm. A controlled environment such as an anechoic chamber, designed to absorb reflections of electromagnetic waves, is the perfect place to avoid multipath and external interference during this characterization.

The function defining the antenna gain is obtained using an access point with an external linearly polarized antenna. Measurements are gathered from a receiver mounted on an automated rotation platform that orients the device in different directions in the azimuth plane. During this process, the application logs the RSSI, accelerometer and compass readings every 1.8° over a full circle. This process is repeated for each device.

To increase our knowledge of the received signal strength gathered through the device, we introduce an RF attenuator to reduce the output power at the transmitter. This mimics the phone being placed at a different distance from the source. Also, we rotated the device in the azimuth plane in a clockwise and counter clockwise manner. These additional steps are key in being able to detect non-linearity in the smartphone's response.

4.2.1 Measurements Analysis

The data gathered, see Fig. 4.1, shows that each device presents a particular antenna pattern. Furthermore, devices of a same type behave alike. Enabling the antenna characterization to be done by device model.

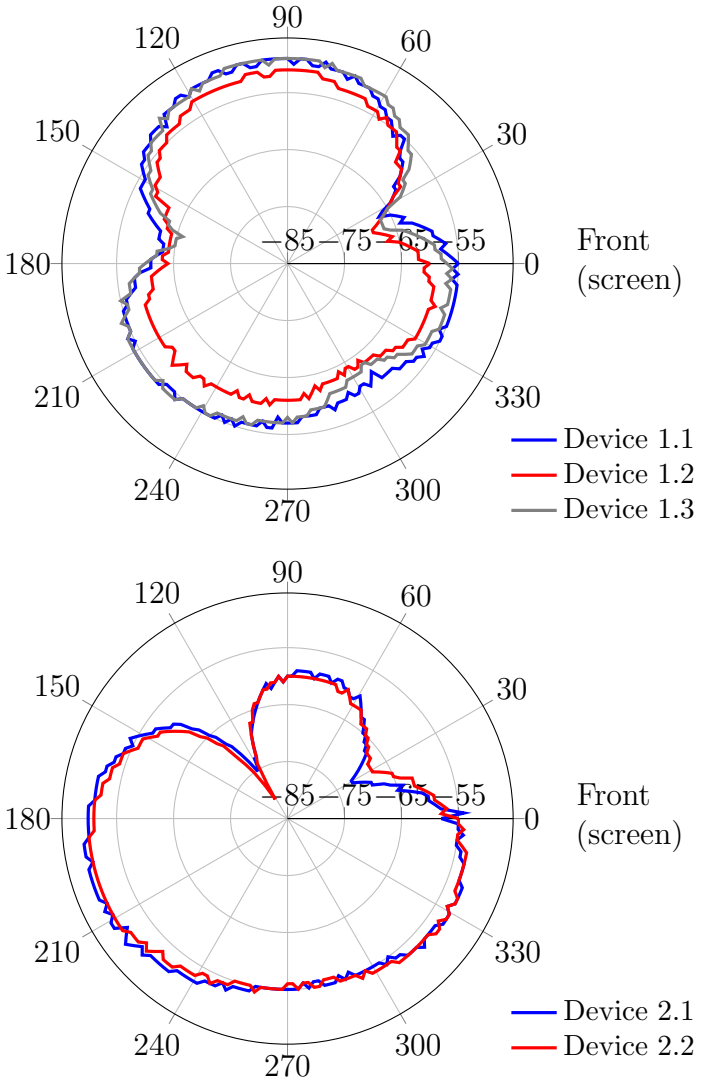

Figure 4.1: This plot shows the antenna gain (dBm) as a function of azimuth angle for two smartphone models (E_θ-polarization, $\theta = 90°$, $0° < \phi < 360°$).

Typically, RSSI is done in the intermediate frequency (IF) stage before the IF amplifier. Additional steps were taken to try to corroborate this assumption and rule out the possibility of confounding effects from an automatic gain control. The latter would be an issue if the RSSI provided by the Android API was being measured after an amplifier. At this case, in the event of a very weak or strong signal, the amplifier would compensate for power, thereby changing the measured antenna behavior. This effect, if present, would have to be taken into account, otherwise the antenna characterization would be misleading for the orientation-aware algorithm. Measurements, including a 30 dB attenuator, reveal that the measured RSSI values are consistent with our hypothesis. That is, the RSSI decreases linearly, preserving antenna behavior, as shown in Fig. 4.2. In the same way, measurements taken in

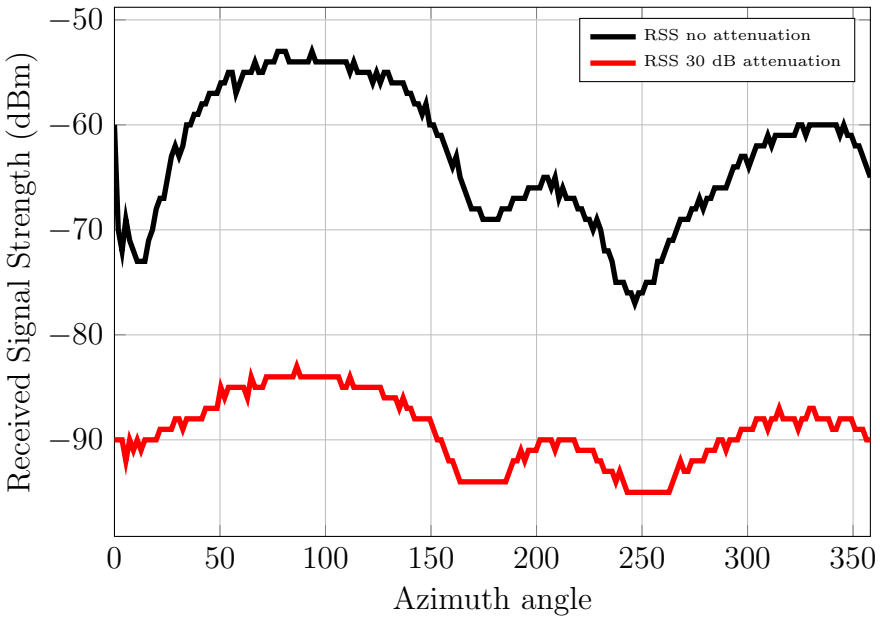

Figure 4.2: This figure shows the antenna behavior with and without a 30dB attenuator attached to the transmitter. The attenuated curve shows two horizontal straight lines when the connection was drop due to low signal strength.

clockwise and counter-clockwise rotation, presented in Fig. 4.3, offer evidence that measurements are memoryless, yielding consistent behavior as desired.

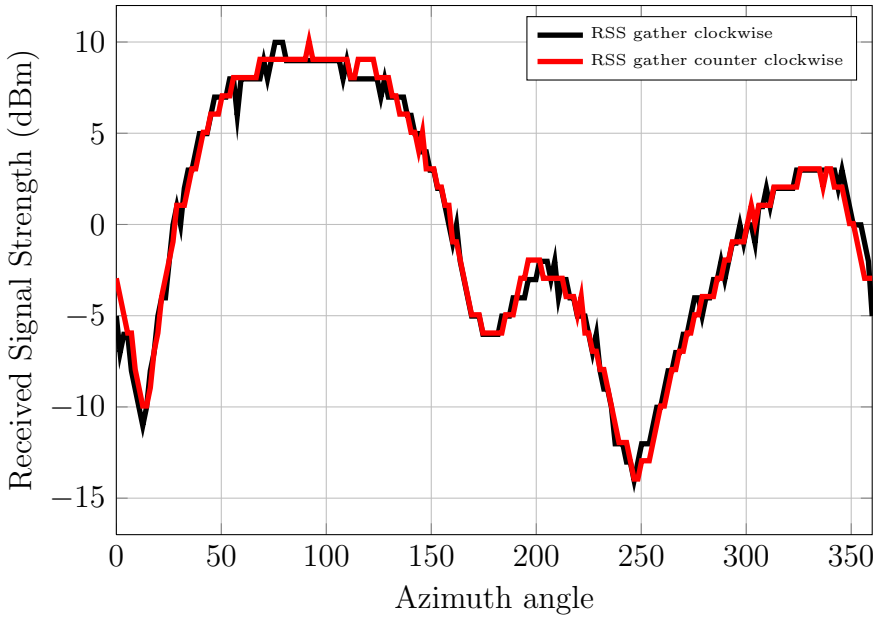

Figure 4.3: This figure shows the normalized antenna behavior for measurements taken in clockwise and counter-clockwise rotation.

4.3 Channel Characterization

The experiment is set in a 100 by 100 meters open field area, which is part of the Texas A&M University campus. Fig. 4.4 offers a satellite image view of the experiment site. The transmitter is place in the middle of this squared area. RSS measurements are taken with the sensing device mounted in a plastic 3D printed structure attached to a PVC section. This aims to avoid potential interference created by the way the phone is being held. It also keeps it at a same height during the entire measurement campaign.

The built-in GPS module, which provides a typical horizontal position accuracy

Figure 4.4: This figure highlights the site used for the experiments and marks the transmitter position for the channel characterization.

Source: Google Earth 7.1.2.2041. (February 25, 2013). 30°37'26.35"N, 96°20'1.42"W, Eye alt 1194 ft. Google 2014. `http://www.earth.google.com` [Accessed February 27, 2014].

of 3 meters in clear sky, makes it capable of recording the geographical positions associated with each sample. This supports a precise distance determination from the source. The measurements were taken around the source at every 45 degrees, with distance ranging from 3 to 70 meters with a single receiver that is moved around several locations. The receiver's relative orientation towards the source is also controlled so that it remains the same during this part of the measurement campaign. This process is repeated with different smartphones for statistical averaging. A heat map of the measurements is shown in Fig. 4.5.

4.3.1 Measurements Analysis

In practice, received signal attenuation involves path loss, large-scale or shadow fading, and small-scale or multipath fading. These effects can be treated as independent processes that combine or superpose to produce an overall fading profile [13].

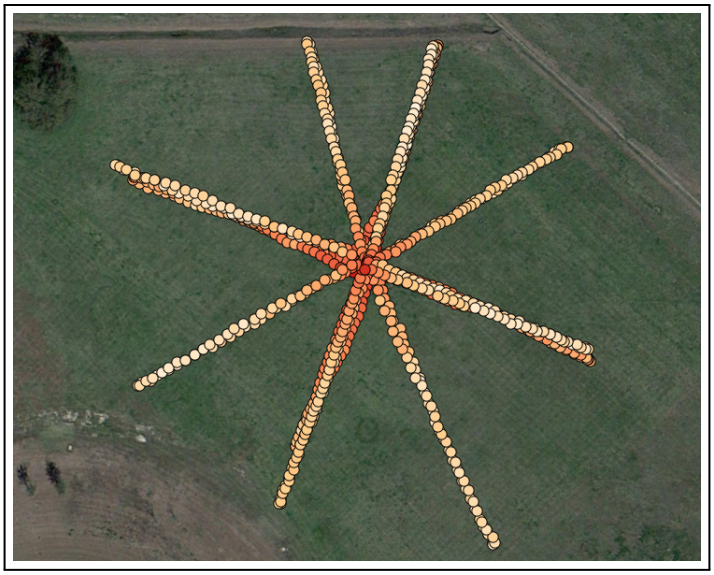

Figure 4.5: Heat map of the training measurements used for the channel characterization.

Several abstract models try to predict the path loss in wireless environments, they are described in the literature. Still the variability and complexity of the radio channel makes it difficult to accurately obtain a deterministic channel model. In such scenarios, statistical models are often used.

In our experiments, we assume that the terrain, vegetation, and presence of large structures in the surroundings result in shadow fading. The immediate vicinities of the transmitter and receiver are unobstructed. This setting minimizes the effects of multipath fading. In this scenario, the statistical log-distance model, with log-normal shadowing, has received much empirical support. It models the variations in received power in outdoors propagation environments [31].

Earlier, in Section 2.1, we described the wireless channel using a combined path loss and shadowing model and presented an equation describing the received signal strength as a function of distance (2.1). The values of A, B and σ_s^2 fully describe the

wireless environment. Parameters A and B can be optimized to minimize the sum of the squares of the error between the model and a wide range of empirical measurements [32]. The difference between the log-distance model and the measurements determine the error variance, σ_s^2.

Herein, the assumption that these errors follow a log-normal distribution [31] is significative. Therefore, we performed a goodness-of-fit test to determine how well a set of experimental data fits a normal model. Test statistics are shown in Table 4.1. One common statistical test for normality, recommended for datasets smaller than 2,000 elements, is the Shapiro-Wilk test where the null hypothesis is that the data is normally distributed and the alternative hypothesis is that the data is not normally distributed. From Table 4.1, the p-value or significance value is 0.724. This value represents the probability of wrongly rejecting the null hypothesis when it is in fact true. Since the p-value value is greater than the level of significance, $\alpha = 0.05$, we can then reject the alternative hypothesis and conclude that the data comes from a normal distribution at the 5% significance level. The Kolmogorov-Smirnov with estimated parameters test also validates this result. The probability distribution shape of the data shows a skewness of -0.104 and kurtosis of -0.047. The skewness quantifies how symmetrical the distribution is, a negative skew indicates an asymmetrical distribution with a long tail to the left. Furthermore, the kurtosis quantifies whether the shape of the data distribution matches the one of a Gaussian distribution, a negative kurtosis means a flatter distribution. Nevertheless, none of these values are substantial and therefore we assume that the error distribution can be treated as Normal. These results can be observed plotting the normalized empirical distribution of the error and a Gaussian distribution with $\sigma = 4.79$, as shown in Fig. 4.6.

The analysis of the data using the least square method defined in (2.4) leads to a system with parameters $\bar{\mathrm{A}} = -47.9$, $\mathrm{B} = -19.5$ and noise level due to shadowing

Table 4.1: This table presents the results from two well-known tests of normality, the Kolmogorov-Smirnov test and the Shapiro-Wilk test, applied to the error between the model and the power measurements.

	Kolmogorov-Smirnov[1]			**Shapiro-Wilk**		
	Statistic	df	p-value	Statistic	df	p-value
Data	0.030	531	0.200[2]	0.998	531	0.724

[1] Lilliefors Significance Correction
[2] This is a lower bound of the true significance.

${\sigma_s}^2 = 24.25$. Figure 4.7 illustrates the received power as a function of distance and the log-distance model. The parameter A that characterizes the channel is given by

$$\mathrm{A} = \bar{\mathrm{A}} - \mathrm{G}_a(\phi) \tag{4.1}$$

where $\bar{\mathrm{A}}$ is the result from the least square approximation and G_a is the gain of the antenna at the relative orientation at which the channel characterization measurements where acquired.

4.4 Localization Campaign

Actual RSSI values, devices global coordinates and orientation are employed to evaluate the performance of the proposed algorithm. This campaign is conducted at the same place mentioned above for the channel characterization experiment. The accuracy of the compass information is critical and so the magnetometer sensor must be calibrated at the beginning of the experiment for better performance. To re-calibrate, the user must move away from external magnetic fields and wave the device in a figure 8 pattern or rotate the phone in all 3 axis.

The localization method being evaluated relies on a distributed network of sensors that measure RSS from a single emitter. The source position is unknown and

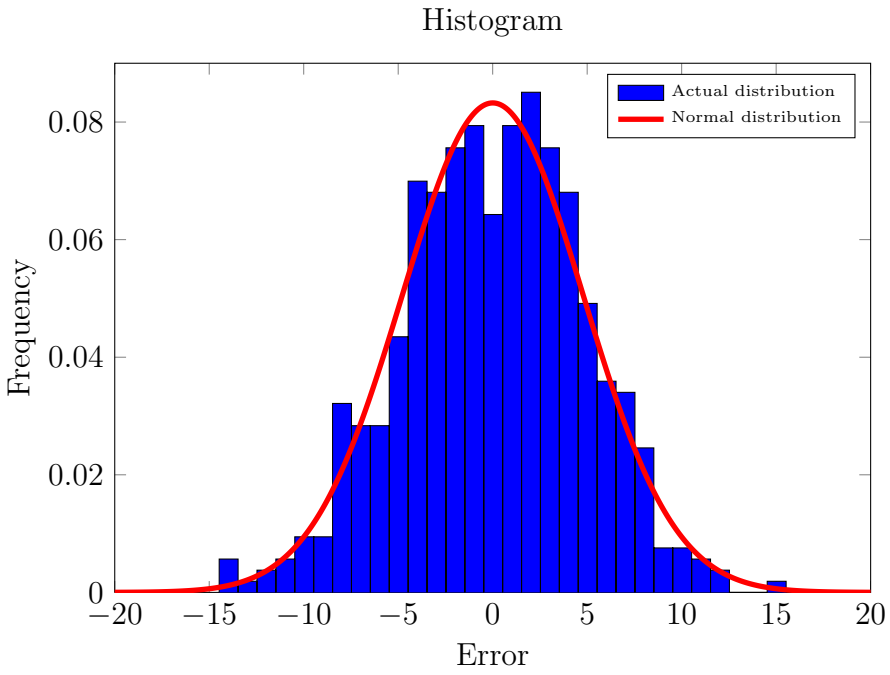

Figure 4.6: Empirical distribution of the error and a theoretical Gauss Distribution with $\sigma = 4.79$.

can be anywhere within the boundaries of the uncertainty area. The locations and orientations of the sensing devices, on the other hand, are known. Several measurements, with random locations and azimuth angles, are taken for each receiver and the procedure is repeated with different smartphones. All measurements gathered are considered independent. Figure 4.8 shows the source and a sample set of data gathered for the evaluation of the algorithm.

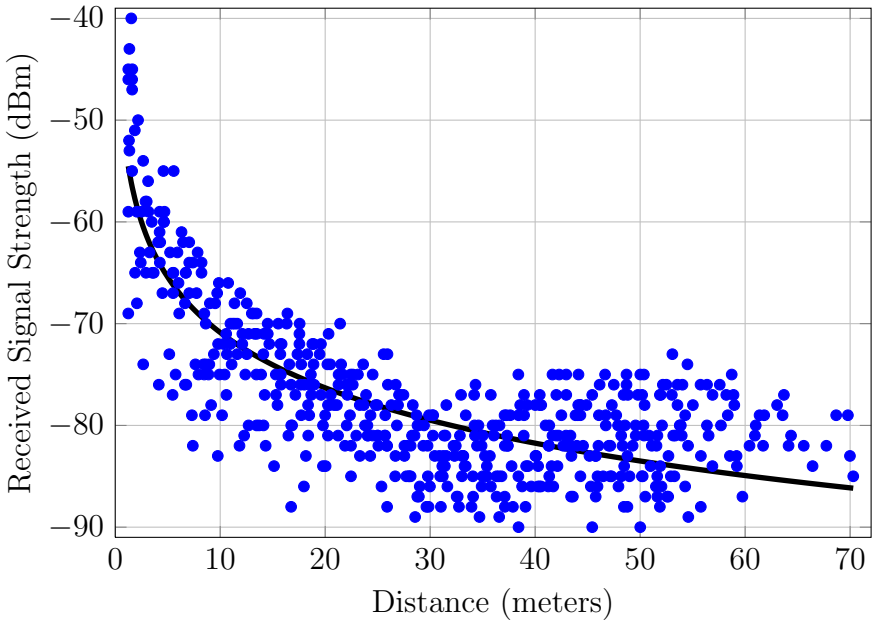

Figure 4.7: Points denote received signal strength as a function of distance from a source in an outdoor suburban environment. The solid line is the least-squares approximation.

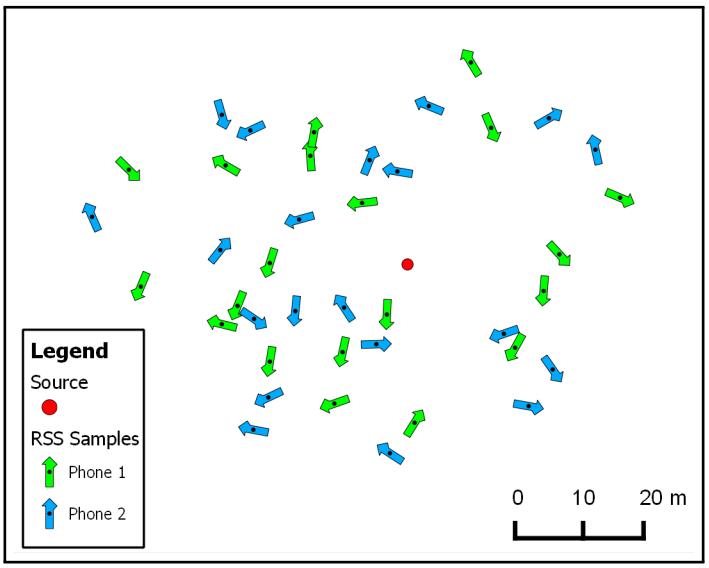

Figure 4.8: This graph illustrates sample data for the evaluation of the algorithm. The source and receivers are represented by red and black circles respectively. Each arrow indicates the smartphone screen direction and colors denote different devices.

5. PERFORMANCE ANALYSIS

Experimental measurements are used to evaluate the performance of the localization algorithm in two ways, numerical simulation and real-life scenarios. To better understand the impact of information asymmetry in localization, we compare the new scheme with the standard setting where the orientation is unknown.

5.1 Numerical Simulation Results

In our numerical simulations, we use the antenna and the channel characterization measurements discussed in Section 4. The area to analyze is a square grid with side length of 100 meters. With a set resolution of one meter, there exist 10,000 possible locations for the source and the sensors. For these simulations, we fix the sensors positions at the corners of the square. In general, the source can be located if and only if at least three sensors do not lie on a line. We randomly generate the azimuth values for all sensors and calculate the received signal strength indicator (RSSI) using the log-normal model from (2.1). To get numerical significance, we run 10,000 trials. Each iteration randomly assigns the source within the grid according to a uniform distribution. The estimated location is obtained using the maximum-likelihood algorithms described in (2.9) and (3.2). The error distance is then computed for each scheme as a function of the number of sensing devices through empirical averaging. A summary of the simulation parameters appears in Table 5.1. Results are shown in Table 5.2. From the latter table, it is clear that the orientation-aware implementation significantly outperforms the standard maximum-likelihood estimator, in terms of distance error. The average distance improvement is about 12.9 meters. The output of one iteration is shown in Fig. 5.1.

In Fig. 5.2, we compare the distributions of the residual distances for the classic

Table 5.1: This table summarizes the simulation parameters.

Parameter	**Value[units]**
Number of iterations	10,000
Number of nodes	3, 4
Uncertainty area	100 x 100 [meters]
A	-47.90 [dBm]
B	-19.50 [dBm]
σ_s^2	7.75 [dBm]
σ_a^2	16.73 [dBm]

Table 5.2: This table lists distance errors as functions of the number of nodes. The orientation-aware implementations perform significantly better than the traditional systems.

Parameter	**Average Error Distance (m)**	
Number of Nodes	Classic Implementation	Orientation Aware Sensors
3	41.11	28.66
4	36.01	22.57

and the orientation-aware implementations. This shows the benefits of the orientation-aware algorithm in terms of accuracy.

The results of the simulations, varying the numbers of receivers, display the maximum likelihood estimator consistency property. The consistency means that, having a sufficiently large number of observations, it is possible to find the source location $\mathbf{x}$ with arbitrary precision. In other words, as the number of receivers goes to infinity the estimator $\hat{\mathbf{x}}$ converges in probability to the true value. From Fig. 5.3, we can appreciate the decrease of the error distance as we increase the number of receivers. We note that for these simulations the receivers' positions do not overlap with one another or with the source. Furthermore, Fig. 5.3 also shows the impact of shadowing variance. Increasing the shadowing variance affects both localization

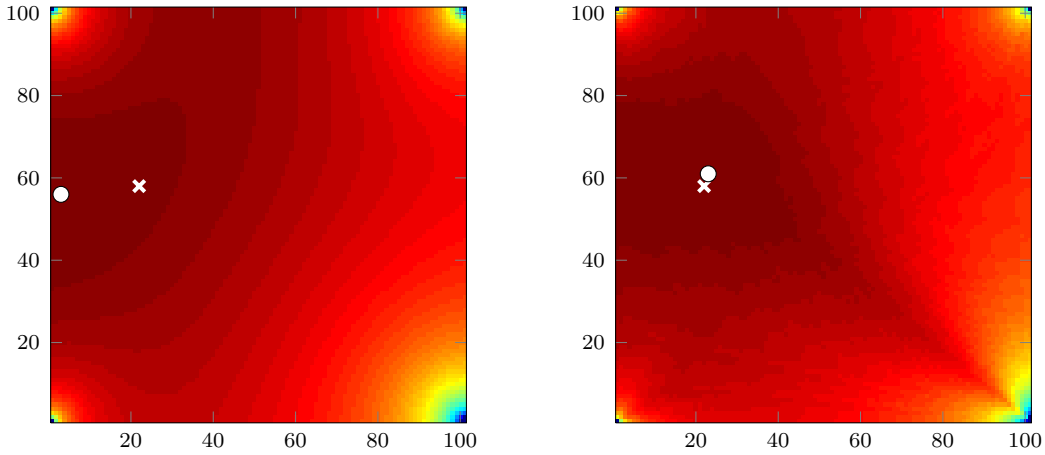

(a) Standard MLE (b) Orientation-Aware MLE

Figure 5.1: Estimated locations obtained using the two MLE algorithms. The source is denoted by x, and the circle represents the estimate.

algorithms, although it seems to have a greater impact on the orientation-aware algorithm.

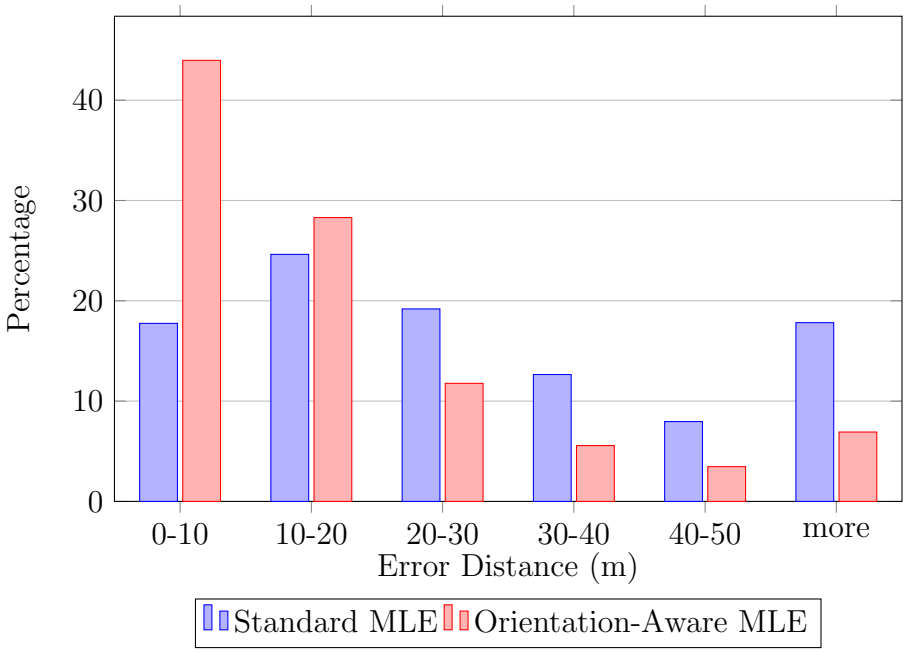

Figure 5.2: Percentage distribution of error distance for a simulation using four receivers.

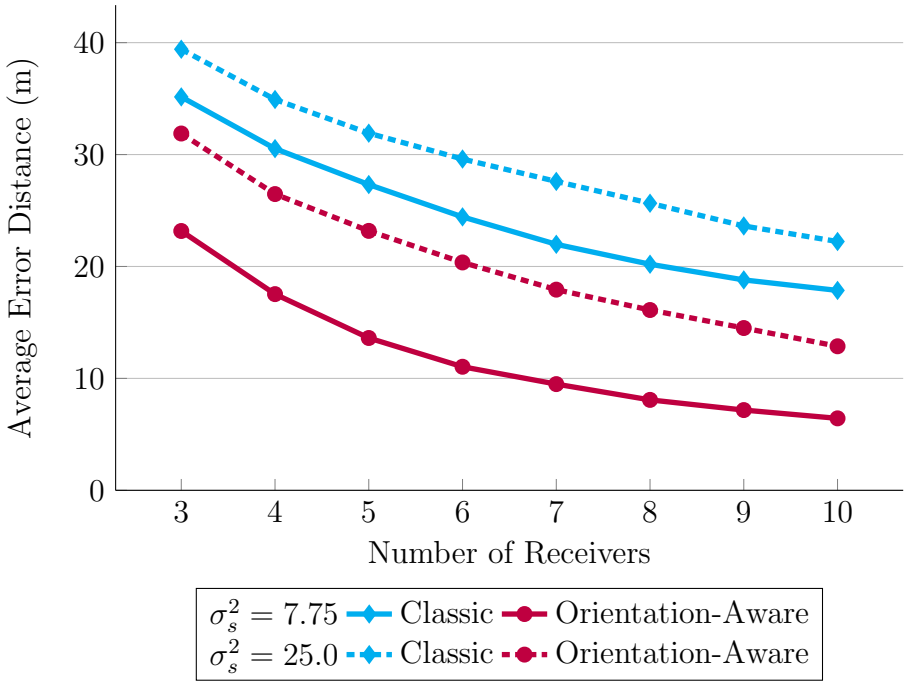

Figure 5.3: The graph showcase the estimation behavior as function of the system parameters.

5.2 Experimental Results

Experimental results, unlike simulations are derived from actual RSSI, GPS positioning and azimuth values obtained directly from the sensing devices. The information is stored in each device locally and later relayed to a central database.

A single localization trial is a combination of samples, depending on the scenario we want to study. We run m choose k trials, where m represents the amount of samples in the data set and k denotes the number of receivers. The parameters used for the algorithm are shown in Table 5.4 and the results are presented in Table 5.5. These values support the notion that increasing the information provided to the algorithm, specifically orientation, leads to a better estimation performance.

A performance comparison of the estimators can be graphically seen in Fig. 5.4. Herein and via similar to simulations, we can appreciate the orientation impact over the estimation process. Likewise, we can observe the error distance reduction as we increase the number of sensing devices. The average unbiased sample variance is summarized in Table 5.3 .

Table 5.3: This table lists the average unbiased sample variance for 3-7 sensing devices as function of the device type.

Node	**Average Unbiased Sample Variance**	
	Classic Implementation	Orientation Aware Sensors
Device 1	199.51	180.69
Device 2	46.55	41.08

Figure 5.5 gives more insight on the precision of both algorithms, showing that the orientation-aware scheme's precision is superior to that of the classic implementation.

Table 5.4: This summarizes the parameters used by the algorithm to evaluate actual RSSI measurements.

Parameter	**Value[units]**
Number of nodes	3, 4, 5
Uncertainty area	100 x 100 [meters]
A	-47.90 [dBm]
B	-19.50 [dBm]
σ_s^2	24.25*, 18.30† [dBm]
σ_a^2	24.96*, 5.62† [dBm]

* Parameter for Device 1

† Parameter for Device 2.

Table 5.5: This table lists distance errors as functions of system parameters for real RSSI measurements.

Parameters		**Average Error Distance (m)**	
Node	Number of Nodes	Classic Implementation	Orientation Aware Sensors
Device 1	3	24.09	21.21
	4	21.31	17.95
	5	19.26	15.29
Device 2	3	15.84	13.83
	4	13.69	11.51
	5	12.06	9.84

(a) Device 1

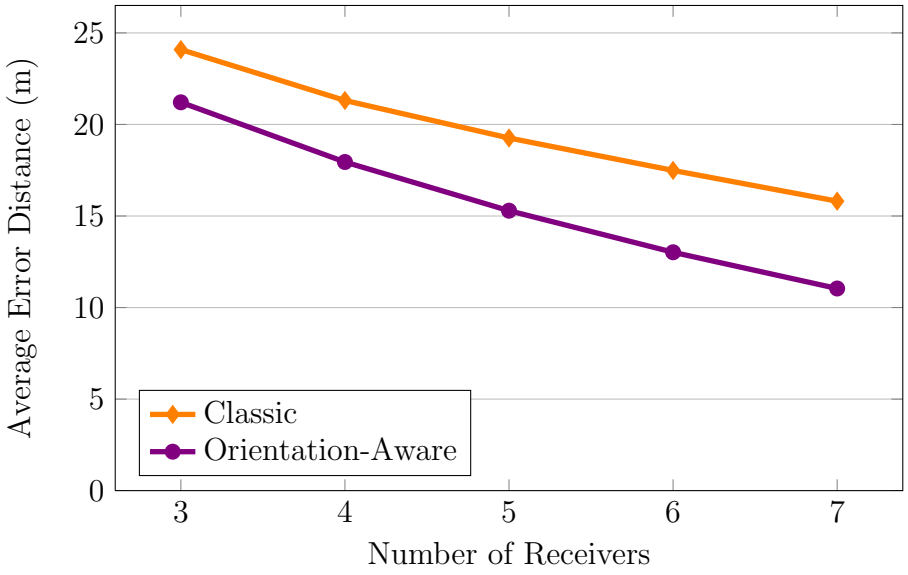

(b) Device 2

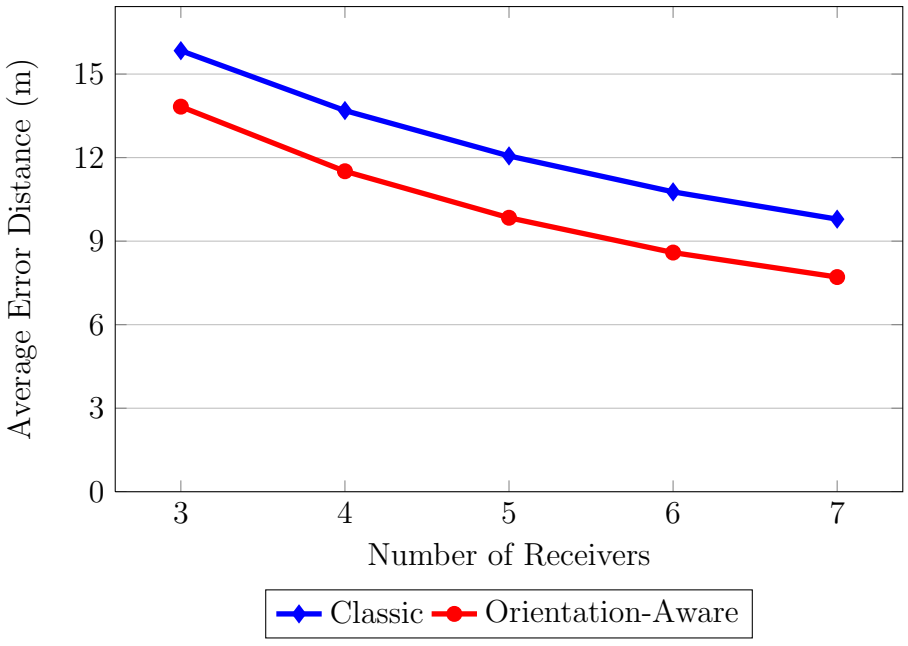

Figure 5.4: Estimation behavior using actual RSSI samples.

Figure 5.6 displays the output of the algorithm for a single trial including 21 receivers. Herein, we can observe the impact of the antenna gain on a heat map. The error distance for the classic implementation is 5 meters. In comparison, the orientation-aware implementation is only 1.5 meters away from the source's true location.

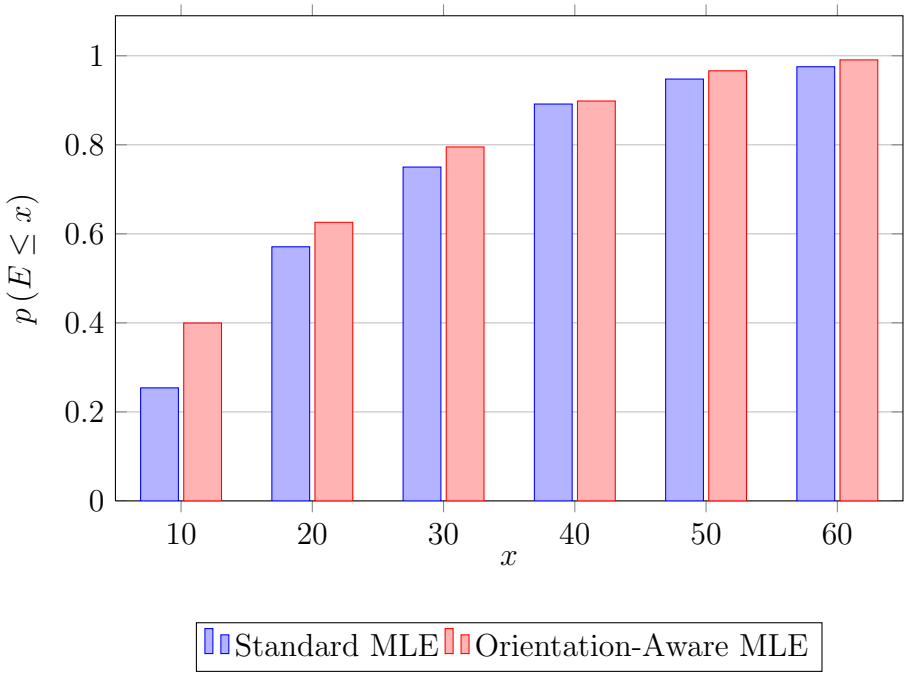

Figure 5.5: Cumulative probability function (CDF) of the distance error using four receivers in a real-world implementation.

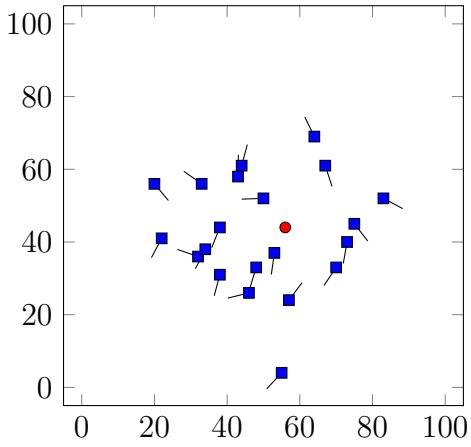

(a) Campaign Setting

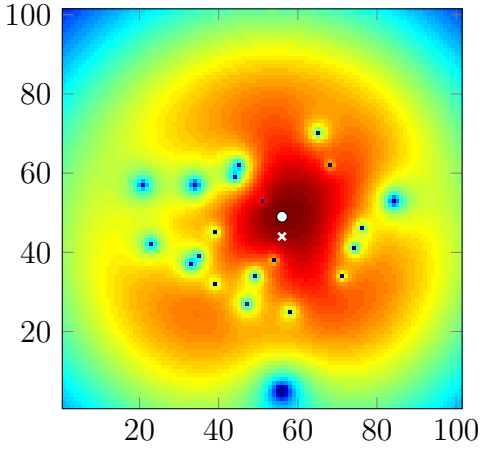

(b) Standard MLE

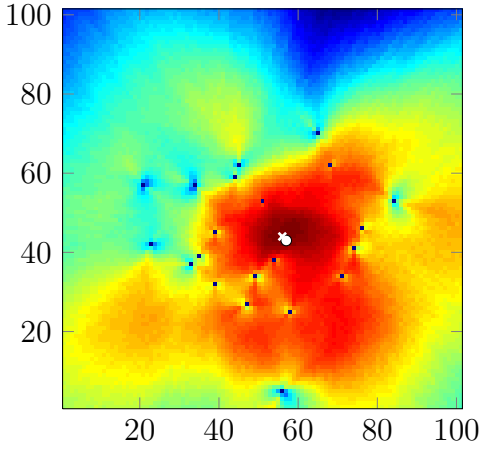

(c) Orientation-Aware MLE

Figure 5.6: Estimated locations obtained using the two MLE algorithms for 21 actual receivers: (a) presents the source's location and the sensors' locations and orientations (azimuth), (b) and (c) show a heat map of the maximum likelihood estimator; the source is denoted by x, and the circle represents the estimate.

6. SUMMARY AND FUTURE RESEARCH

In this thesis, we report on the opportunity to enhance the performance of a localization system by incorporating orientation information. We employed Android smartphones as sensing devices and tested the feasibility of using current embedded microelectromechanical sensors to characterize orientation. Although successful, several challenges such as compass recalibration and sensor behavior considerations have to be taken into account. We also studied the antenna radiation characteristics of different devices and demonstrated that antenna patterns are consistent between smartphones of a same model. In contrast, they are distinct across different models. This presents a challenge for an orientation-aware algorithm because device-dependent antenna patterns must be measured and stored.

A new algorithm that leverages the spherical asymmetry of typical antenna radiation patterns and the devices knowledge of its orientation is introduced. We analyzed through simulations and experiments the overall system performance of the new orientation-aware scheme. Using average error distance as a system performance metric, we demonstrated that the orientation-awareness of the sensing device has a positive effect on the accuracy of an RSS-based localization system. Notably, the orientation-aware implementation demonstrated tangible gains in real systems, outperforming a standard maximum-likelihood estimator.

Although the real-world test was performed in a controlled environment, given that it was set to avoid multipath and human presence during the localization process, we hope these results provide good insight into the capabilities of orientation-aware device and expect that this idea can be extended to other systems in the context of communication such as interference management, precoding MIMO selec-

tion, scheduling and hybrid networks.

This work can be extended by implementing an algorithm that uses a three dimensional characterization of both the antenna pattern and the orientation of the sensing device. Also, different computationally attractive methods for computing estimation can be incorporated. Above all, the goal would be to incorporate considerations of real-life implementation such as localization under human presence conditions and non-controlled environments where multipath fading may exist, to prove the viability of applying this type of algorithms in practical communication systems.

REFERENCES

[1] H. Wymeersch, J. Lien, and M. Win, "Cooperative localization in wireless networks," *Proceedings of the IEEE*, vol. 97, no. 2, pp. 427–450, 2009.

[2] J. A. Costa, N. Patwari, and A. O. Hero III, "Distributed weighted-multidimensional scaling for node localization in sensor networks," *ACM Transactions on Sensor Networks*, vol. 2, no. 1, pp. 39–64, 2006.

[3] M. Rudafshani and S. Datta, "Localization in wireless sensor networks," in *Proceedings of the 6th International Conference on Information Processing in Sensor Networks, IPSN 2007*. ACM, 2007, pp. 51–60.

[4] Z. Hu and B. Li, "Fundamental performance limits of wireless sensor networks," *Ad Hoc and Sensor Networks*, pp. 81–101, 2004.

[5] Y. Al-Obaisat and R. Braun, "On wireless sensor networks: Architectures, protocols, applications, and management," in *Proceedings of the 1st IEEE International Conference on Wireless Broadband and Ultra Wideband Communication, AusWireless 2006*, 2006.

[6] S. V. Schell and W. A. Gardner, "High-resolution direction finding," in *Handbook of Statistics*, N. K. Bose and C. Rao, Eds., vol. 10. Netherlands: Elsevier Science Publishers B.V., 1993, pp. 755–817.

[7] National Oceanic and Atmospheric Administration (NOAA), "Emergency beacons," accessed April 9, 2014. [Online]. Available: www.sarsat.noaa.gov/emerbcns.html

[8] N. Patwari, J. Ash, S. Kyperountas, A. Hero, R. Moses, and N. Correal, "Locating the nodes: Cooperative localization in wireless sensor networks," *IEEE*

Signal Processing Magazine, vol. 22, no. 4, pp. 54–69, 2005.

[9] A. Sayed, A. Tarighat, and N. Khajehnouri, "Network-based wireless location: Challenges faced in developing techniques for accurate wireless location information," *IEEE Signal Processing Magazine*, vol. 22, no. 4, pp. 24–40, 2005.

[10] M. Chryssomallis, "Smart antennas," *IEEE Antennas and Propagation Magazine*, vol. 42, no. 3, pp. 129–136, 2000.

[11] P. Farago, "iOS and Android Adoption Explodes Internationally," Flurry, 2012, accessed January 25, 2014. [Online]. Available: blog.flurry.com/bid/88867/iOS-and-Android-Adoption-Explodes-Internationally

[12] Cisco Systems, Inc., "Cisco visual networking index: Global mobile data traffic forecast update, 2013–2018," accessed April 10, 2014. [Online]. Available: www.cisco.com/c/en/us/solutions/collateral/service-provider/visual-networking-index-vni/white_paper_c11-520862.html

[13] A. Goldsmith, *Wireless Communications*. United Kingdom: Cambridge University Press, 2005.

[14] A. Domazetovic, L. J. Greenstein, N. B. Mandayam, and I. Seskar, "Propagation models for short-range wireless channels with predictable path geometries," *IEEE Transactions on Communications*, vol. 53, no. 7, pp. 1123–1126, 2005.

[15] R. Stoleru, T. He, and J. A. Stankovic, "Range-free localization," in *Secure Localization and Time Synchronization for Wireless Sensor and Ad Hoc Networks*, R. Poovendran, C. Wang, and S. Roy, Eds. New York: Springer, 2007, vol. 30, pp. 3–31.

[16] C. Tran-Xuan and I. Koo, "An rss-based localization scheme using direction calibration and reliability factor information for wireless sensor networks." *KSII*

Transactions on Internet & Information Systems, vol. 4, no. 1, 2010.

[17] C. Tang and J. Yin, "A localization algorithm of weighted maximum likelihood estimation for wireless sensor networks," *Journal of Information & Computational Science*, vol. 8, no. 16, pp. 4293–4300, 2011.

[18] N. Salman, A. Kemp, and M. Ghogho, "Low complexity joint estimation of location and path-loss exponent," *IEEE Wireless Communications Letters*, vol. 1, no. 4, pp. 364–367, 2012.

[19] J. C. Liberti and T. S. Rappaport, *Smart Antennas for Wireless Communications: IS-95 and Third Generation CDMA Applications.* New Jersey: Prentice Hall PTR, 1999.

[20] S. Zekavat, A. Kolbus, X. Yang, Z. Wang, J. Pourrostam, and M. Pourkhaatoun, "A novel implementation of doa estimation for node localization on software defined radios: Achieving high performance with low complexity," in *IEEE International Conference on Signal Processing and Communications, ICSPC 2007*, 2007, pp. 983–986.

[21] I. Ziskind and M. Wax, "Maximum likelihood localization of multiple sources by alternating projection," *IEEE Transactions on Acoustics, Speech and Signal Processing*, vol. 36, no. 10, pp. 1553–1560, 1988.

[22] R. Roy, A. Paulraj, and T. Kailath, "Esprit–a subspace rotation approach to estimation of parameters of cisoids in noise," *IEEE Transactions on Acoustics, Speech and Signal Processing*, vol. 34, no. 5, pp. 1340–1342, 1986.

[23] R. Schmidt, "Multiple emitter location and signal parameter estimation," *IEEE Transactions on Antennas and Propagation*, vol. 34, no. 3, pp. 276–280, 1986.

[24] V. Madisetti, Ed., *Wireless, Networking, Radar, Sensor Array Processing, and Nonlinear Signal Processing*, ser. The Digital Signal Processing Handbook, Second Edition. Florida: Taylor & Francis, 2010.

[25] P. Gao, W. Shi, W. Zhou, H. Li, and X. Wang, "A location predicting method for indoor mobile target localization in wireless sensor networks," *International Journal of Distributed Sensor Networks*, 2013.

[26] Y.-T. Chan, H. Yau Chin Hang, and P.-C. Ching, "Exact and approximate maximum likelihood localization algorithms," *IEEE Transactions on Vehicular Technology*, vol. 55, no. 1, pp. 10–16, 2006.

[27] J. Fessler and A. Hero, "Space-alternating generalized expectation-maximization algorithm," *IEEE Transactions on Signal Processing*, vol. 42, no. 10, pp. 2664–2677, 1994.

[28] F. de Leon and J. Marciano, J.J.S., "Application of music, esprit and sage algorithms for narrowband signal detection and localization," in *TENCON 2006. 2006 IEEE Region 10 Conference*, 2006, pp. 1–4.

[29] G. Lui, T. Gallagher, B. Li, A. G. Dempster, and C. Rizos, "Differences in rssi readings made by different wi-fi chipsets: A limitation of wlan localization," in *International Conference on Localization and GNSS, ICL-GNSS 2011*, 2011, pp. 53–57.

[30] B. Rolfe, S. Ekanayake, P. Pathirana, and M. Palaniswami, "Localization with orientation using rssi measurements: Rf map based approach," in *3rd International Conference on Intelligent Sensors, Sensor Networks and Information, ISSNIP 2007*. IEEE, 2007, pp. 311–316.

[31] T. S. Rappaport *et al.*, *Wireless Communications: Principles and Practice*. New Jersey: Prentice Hall PTR, 1996, vol. 2.

[32] T. K. Moon and W. C. Stirling, *Mathematical Methods and Algorithms for Signal Processing*. New Jersey: Prentice Hall, 2000.

[33] G. Casella and R. L. Berger, *Statistical Inference*, 2nd ed. California: Duxbury Thomson Learning, 2001.

[34] V. Honkavirta, T. Perala, S. Ali-Loytty, and R. Piche, "A comparative survey of wlan location fingerprinting methods," in *6th Workshop on Positioning, Navigation and Communication, WPNC 2009*, 2009, pp. 243–251.

[35] S. Ayub, A. Bahraminisaab, and B. Honary, "A sensor fusion method for smart phone orientation estimation," in *Proceedings of the 13th Annual Post Graduate Symposium on the Convergence of Telecommunications, Networking and Broadcasting, Liverpool*, 2012.

[36] National Oceanic and Atmospheric Administration (NOAA), "Wandering of the geomagnetic poles," accessed March 10, 2014. [Online]. Available: www.ngdc.noaa.gov/geomag/GeomagneticPoles.shtml